1-10-1975

Single-Domain Grain Size Limits for Metallic Iron

Robert F. Butler
University of Portland, butler@up.edu

Subir K. Banerjee

Single-Domain Grain Size Limits for Metallic Iron

ROBERT F. BUTLER[1] AND SUBIR K. BANERJEE

Department of Geology and Geophysics, University of Minnesota
Minneapolis, Minnesota 55455

Theoretical examination of possible nonuniform spin configurations in metallic iron indicates that circular spin (CS) is the lowest-energy nonuniform arrangement. The upper grain size limit (d_0) to single-domain (SD) behavior is thus defined by the SD to CS transition. Superparamagnetic (SP) behavior marks the lower grain size limit to the stable SD range, and the SP to SD threshold size (d_s) can be determined by Néel's relaxation theory. Calculations of d_0 and d_s for spherical metallic iron particles at 290°K indicate that d_0 (=173 Å) $< d_s$ (=260 Å), and no stable SD range exists. A stable SD range does exist for prolate ellipsoids of elongation $q > 1.1$ but remains very constricted. For a prolate ellipsoid of $q = 1.67$, a stable SD range occurs between the SP critical length $l_s = 150$ Å and $d_0 = 360$ Å. Both d_0 and d_s increase with temperature, but the stable SD range decreases. The size and shape criteria for the stable SD behavior of metallic iron help to explain (1) the low SD content of lunar samples, (2) the widespread occurrence of SP behavior and viscous magnetization in lunar soils and low metamorphic grade breccias, (3) the changes in the magnetic properties of breccias during annealing, and (4) the increased SD content of shocked breccias. The narrow grain size limits for SD behavior also suggest that magnetostatic interaction between metal grains in the solar nebula is not a viable mechanism for iron-silicate fractionation.

The importance of stable single-domain (SD) grains to rock magnetism has been recognized for some time, primarily because of the very high efficiency of SD grains in carrying thermoremanent magnetization, in terms of both magnitude and stability of remanence [*Néel*, 1955]. Particles with parallel alignment of atomic magnetic moments throughout the entire grain volume are defined as SD. Each SD particle has an associated relaxation time over which its magnetization is stable. In SD grains below a critical size, thermal agitation of the magnetic moment destroys the remanence-carrying capability of the grain. This behavior is known as superparamagnetism. The SD grains above the critical size are called stable SD's since their relaxation times range from several minutes up to geologic times. The grain size at which the stable SD to superparamagnetic (SP) transition occurs is called d_s. The upper grain size limit to SD behavior is imposed by transition to a nonuniform spin structure in which the atomic magnetic moments are no longer parallel throughout the particle. This transition is caused by the very high magnetostatic energy of SD grains and takes place at a critical size known as d_0. Thus stable SD behavior is observed only within the range $d_s < d < d_0$. Although particles with $d > d_0$ do carry remanent magnetization, their remanence is much lower in both magnitude and stability than the remanence in SD grains. Thus determination of the stable SD grain size range is accomplished by determining the upper and lower grain size limits, d_0 and d_s, respectively.

Because of the obvious importance of fine-grained magnetite in carrying the natural remanent magnetization (NRM) of terrestrial volcanic rocks, a great deal of effort has been expended to delineate the stable SD grain size range for magnetite. Recent experimental determinations of d_s and d_0 for magnetite [*Dunlop*, 1972, 1973] compare favorably with theoretical estimates [*Evans*, 1972; *Butler and Banerjee*, 1975]. However, the importance of determining the stable SD grain size range in metallic iron has only recently become apparent. This interest is due primarily to the discovery that NRM in the lunar samples is carried by fine metallic iron particles

[*Strangway et al.*, 1972; *Fuller*, 1974]. It is generally, albeit only qualitatively, recognized that the stable SD grain size range for metallic iron is much narrower and occurs at a much smaller size than that for magnetite [*Brown*, 1968; *Morrish*, 1965, p. 342]. In fact, it is commonly stated that the SD range is from 150 to 300 Å in diameter for spherical particles. However, a rigorous and thorough theoretical examination of the stable SD grain size range for metallic iron as a function of grain shape and temperature has not been undertaken. In view of the many experimental problems such as viscous magnetization [*Gose et al.*, 1972; *Nagata et al.*, 1972] and chemical and grain size changes during heating [*Grommé and Doell*, 1971; *Pearce et al.*, 1972] that have been encountered in studying magnetic properties of lunar samples, determination of the SD range for metallic iron evolves as an important problem in lunar science.

Another incentive for calculating the stable SD grain size range comes from the cosmochemical problem of iron-silicate fractionation in the early solar nebula. *Larimer and Anders* [1970] and *Grossman and Larimer* [1974] have pointed out that the temperature at which the fractionation took place is very near the Curie temperature of the Fe-Ni alloy grains in chondritic meteorites. Thus the possibility arises that the iron-silicate fractionation is triggered by the onset of ferromagnetism in the metallic grains. *Harris and Tozer* [1967] suggested that magnetostatic interaction of the metallic grains could provide the required mechanism. However, their formulation applies to SD particles only [*Banerjee*, 1967]. Therefore determining the stable SD grain size range for metallic iron in the temperature range of iron-silicate fractionation will help in evaluating the applicability of the magnetostatic interaction mechanism of *Harris and Tozer* [1967].

Since fine particles of iron tend to form in ellipsoids of revolution rather than to be bounded by crystal faces, we will consider spherical particles and prolate ellipsoids of various elongation. The theory of SP threshold calculations and SD to nonuniform spin threshold calculations will first be introduced. The stable SD grain size range for metallic iron will then be delineated by calculations of the lower and upper limits, d_s and d_0, respectively. Results of these calculations will be followed by a discussion of the implications for lunar magnetism and iron-silicate fractionation in the solar nebula.

---

[1] Now at Department of Geosciences, University of Arizona, Tucson, Arizona 85721.

SP THRESHOLD d_s

The lower limit to stable SD behavior imposed by the transition to superparamagnetism can be calculated by employing Néel's [1955] relaxation equation:

$$\tau = f_0^{-1} \exp(vh_cJ_s/2kT) \qquad (1)$$

where τ is the relaxation time (in seconds), f_0 is the frequency factor ($\sim 10^9$/s for iron), v is the grain volume (in cubic centimeters), h_c is the particle coercive force (in oersteds), J_s is the saturation magnetization (in emu/cm³), k is Boltzmann's constant, and T is the absolute temperature (in degrees Kelvin). This equation was derived by Néel for fine particles with uniaxial anisotropy. The factor $(vh_cJ_s/2kT)$ in (1) is the energy barrier that the magnetic moment must surmount to spontaneously reverse. Thus (1) can be rewritten to give [Bean and Livingston, 1959]

$$\tau = f_0^{-1} \exp(E_B/kT) \qquad (2)$$

where E_B is the energy barrier for reversal of magnetic moment. Equation (2) applies to particles with either cubic or uniaxial anisotropy.

For spherical iron particles the energy barrier between easy directions of magnetization is produced by magnetocrystalline anisotropy. When the magnetic moment flips between adjacent [100] easy directions of magnetization, it must go over the energy barrier supplied by the magnetocrystalline anisotropy energy in the [110] direction. Thus the energy barrier in (2) for spherical iron particles is $(K_1v/4)$, where K_1 is a first-order magnetocrystalline anisotropy constant. The relaxation equation becomes

$$\tau = f_0^{-1} \exp(K_1v/4kT) \qquad (3)$$

The SP threshold size as a function of temperature, $d_s(T)$, can be calculated by substituting a critical relaxation time τ_s for SP behavior into (3) and solving to give

$$d_s(T) = \{[24kT/\pi\ K_1(T)]\ [\ln\ (f_0\tau_s)]\}^{1/3} \qquad (4)$$

For prolate ellipsoids the anisotropy is uniaxial and is supplied by shape anisotropy. The resulting particle coercive force is

$$h_c = \Delta N J_s \qquad (5)$$

where ΔN is the difference between the self-demagnetizing factors of the equatorial axis a and the polar axis b. Self-demagnetizing factors are easily calculated for prolate ellipsoids of various elongations, $q = b/a$, as shown by Morrish [1965, p. 10]. Substituting (5) into (1) and solving for the threshold length $l_s(T)$ yield

$$l_s(T) = \{[12q^2kT/\pi\ \Delta N J_s^2(T)][\ln\ (f_0\tau_s)]\}^{1/3} \qquad (6)$$

Rigorous derivation of the frequency factor f_0 for uniaxial anisotropy by Brown [1963] has shown that f_0 is a function of v, h_c, J_s, and T. Inclusion of the volume dependence of f_0 in (4) and (6) leads to very untidy transcendental equations for SP threshold size. However, as was pointed out by Dunlop and West [1969], this refinement of the relaxation equation is of limited importance to calculations of d_s. For example, for a spherical iron particle at room temperature ($\tau_s = 100$ s), $d_s = 258$ Å when $f_0 = 10^9$/s and $d_s = 266$ Å when $f_0 = 10^{10}$/s. Thus a constant frequency factor of 10^9/s will be used here. It is interesting to note, however, that a rigorous derivation of f_0 for cubic anisotropy and relaxation times of $>10^{-6}$ s is extremely difficult and has not yet been accomplished [Aharoni, 1973].

METHOD OF d_0 CALCULATION

The upper limit to SD behavior, d_0, is more difficult to predict theoretically than the SP threshold because there are many possible nonuniform configurations that must be considered. Therefore the nature of the upper limit to SD behavior will depend on the mineral in question. The particular nonuniform configuration that does develop at d_0 (presumably the lowest-energy configuration) is very important. One must know what the preferred configuration is in order to calculate the threshold grain size d_0.

Rigorously determined upper and lower bounds for d_0 have been derived by micromagnetics theory [Brown, 1968]. For grain sizes less than the lower limit, the SD configuration must be the lowest-energy spin arrangement. Conversely, for grains larger than the upper bound derived from micromagnetics, a nonuniform spin configuration must be the lowest-energy arrangement. Therefore we can use micromagnetics to provide limits within which d_0 must fall. However, micromagnetics theory is not able to tell us what the lowest-energy nonuniform configuration will be.

The lower bound occurs at a critical radius a_{c0}, given by Brown [1968] as

$$a_{c0} = (3.6055/J_s)(A/2\pi)^{1/2} \qquad (7)$$

where A is the exchange constant. The upper bound occurs at a critical radius a_{c1}, given by

$$a_{c1} = [(4.5292)(A/2\pi)^{1/2}]/[J_s]\ [1.0 -$$
$$(5.615)(K_1/4J_s^2)]^{1/2} \qquad (8)$$

Any theoretically derived value of d_0 that is proposed as the upper limit to SD behavior must fall within the limits defined by micromagnetics theory.

A search of the available literature has revealed three spin arrangements that are candidates for the lowest-energy nonuniform configuration in metallic iron. These configurations are (1) magnetization curling [Frei et al., 1957; Brown, 1968],
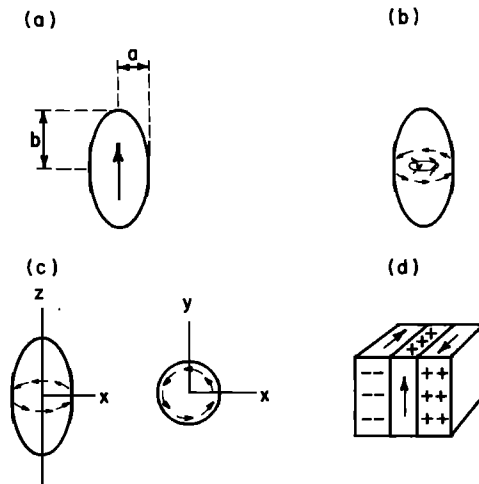

Fig. 1. The SD and nonuniform spin configurations. (a) The SD configuration in which all atomic magnetic moments are parallel. Semimajor axis b and semiminor axis a are also illustrated. (b) The magnetization curling arrangement. The component of magnetization parallel to the polar axis decreases with distance from the axis, and the circumferential component increases. (c) The CS configuration. The atomic magnetic moments curl about the polar axis and describe circles in the equatorial plane. (d) The two-domain plus 180° wall configuration. The arrows show the directions of magnetization in the two domains and in the wall. The magnetic charge distribution is also shown.

(2) circular spin (CS) [*Morrish,* 1965, p. 342; *Frei et al.,* 1957], and (3) two-domain plus 180° domain wall [*Amar,* 1957, 1958*a, b*]. The magnetization curling arrangement is shown in Figure 1*b*. In this configuration the component of magnetization along the polar axis of the particle decreases with distance from the axis. The circumferential component increases with distance from the polar axis. Thus magnetization curling involves magnetostatic, magnetocrystalline, and exchange energies. Although the configuration appears complex, the energies involved can be calculated without assumptions or approximations. *Brown* [1968] used the magnetization curling configuration to calculate the upper bound critical radius a_{c1} given by (8). He chose the magnetization curling mode for calculation of the upper bound not because curling is necessarily the lowest-energy nonuniform configuration but because the energies involved could be calculated rigorously.

Morrish [1965, p. 342] and *Frei et al.* [1957] have considered the CS configuration (Figure 1*c*). For CS the atomic moments curl about the polar axis of the particle and describe circles in the equatorial plane. There are no free magnetic poles for this configuration, and therefore CS has the advantage that there is no magnetostatic energy involved. There is, of course, considerable exchange energy in this configuration. However, several assumptions and approximations are necessary to calculate the energy of the CS arrangement.

The first approximation is that magnetocrystalline anisotropy energy can be neglected. At d_0 the energy density (energy per unit volume) of the SD particle would be equal to the energy density of the CS configuration. Thus we can evaluate the validity of neglecting magnetocrystalline energy by comparing the energy density of a SD particle with the maximum energy density that could arise from magnetocrystalline anisotropy. The energy density of a SD particle, e_{SD}, is

$$e_{SD} = \tfrac{1}{2}NJ_s^2 \qquad (9)$$

where N is the self-demagnetizing factor. For a spherical iron particle, $N = 4\pi/3$ and $J_s = 1720$ emu/cm³, and $e_{SD} = 6.2 \times 10^6$ ergs/cm³. The maximum energy density from magnetocrystalline anisotropy, e_K, would occur if the entire particle was magnetized along a hard direction of magnetization. For iron this would be the [111] direction, and e_K would be given by

$$e_K[111] = K_1/3 \qquad (10)$$

For metallic iron, $K_1 = 4.5 \times 10^5$ ergs/cm³ and $e_K[111] = 1.5 \times 10^5$ ergs/cm³. Thus $e_{SD} \gg e_K[111]$, and the approximation that magnetocrystalline energy can be neglected in deriving the energy of the CS configuration is valid.

The second assumption involved occurs when the exchange energy of the CS arrangement is derived. As *Morrish* [1965, p. 343] pointed out, a mathematical singularity in the expression for exchange energy arises at the center of the particle. This singularity simply reflects the fact that the direction of the magnetic moment of the central atom is indeterminate. This problem is more mathematical than physical. The local high exchange energy of a contorted spin arrangement along the polar axis of the particle will add little to the toal exchange energy of the particle since the volume fraction involved is minute. Thus Morrish neglects the exchange energy of the atoms along the polar axis and integrates the total exchange energy by placing the lower limit of integration one lattice spacing away from the polar axis.

Given these two reasonable approximations, *Morrish* [1965, p. 342] compares the exchange energy of the CS configuration

with the magnetostatic energy of a SD configuration. The critical semiminor axis a_0 at which the SD to CS transition will occur is given by the transcendental equation

$$a_0^2/[\ln (2a_0/c) - 1.0] = 6J_eS^2/cN_bJ_s^2 \qquad (11)$$

where c is the lattice constant (2.9 Å for metallic iron), J_e is the exchange integral, S is the total spin quantum number per atom (1 for iron), and N_b is the self-demagnetizing factor along the polar axis. Although there is not complete agreement on the value of the exchange constant A for metallic iron, there is much less agreement on the value of the exchange integral J_e. Thus, rather than estimate J_e from the Curie temperature, as was suggested by *Morrish* [1965, p. 283], we prefer to substitute $A = 2J_eS^2/c$ [*Chikazumi,* 1964, p. 189] into (11) to give

$$a_0^2/[\ln (2a_0/c) - 1.0] = 3A/N_bJ_s^2 \qquad (12)$$

Amar [1957, 1958*a, b*] suggested that the upper limit to SD behavior would be imposed by transition to a two-domain plus 180° wall configuration (Figure 1*d*). Amar's treatment involves two refinements of *Kittel's* [1949] attempts to determine d_0 by a similar method. Amar considered the energy dependence of the 180° wall on the wall thickness and included the magnetostatic energy of the spins in the wall itself. Both of these factors were neglected by Kittel. The technique amounts to assuming that a particle of a given size d contains a 180° wall and allowing the wall to adjust its width so as to minimize the energy of the two-domain configuration. The critical size d_0 is determined by the particle size at which the total energy of the two-domain configuration drops below that of a SD particle of equal size. The domain wall energy in bulk material, σ_0, and the wall width in bulk material, δ_0, are necessary input parameters in Amar's technique. For these quantities we have used the values $\sigma_0 = 1.25$ ergs/cm² and $\delta_0 = 1413$ Å for a 180° domain wall parallel to (100) and $\sigma_0 = 1.72$ ergs/cm² and $\delta_0 = 727$ Å for a 180° wall parallel to (110) [*Lilley,* 1950; *Stoner,* 1950]. Amar's technique applies strictly to parallelepiped-shaped particles only. However, since the self-demagnetizing factors for a cube and a sphere are equivalent, comparison of the predicted d_0 for a cubic iron particle should give us a good estimate of the d_0 for the two-domain configuration in a spherical particle.

RESULTS

Although the ferromagnetic properties of metallic iron have been investigated for many years, agreement on the value of the exchange constant A has not been reached. The range of reported values is from 0.3×10^{-6} erg/cm [*Wohlfarth,* 1952] to 2×10^{-6} erg/cm [*Kittel,* 1949]. Given this uncertainty, we have used $A = 10^{-6}$ erg/cm as a representative value in calculating the d_0 thresholds for spherical iron particles given in Table 1. This table compares the d_0 threshold grain sizes predicted by the three nonuniform spin configurations under consideration. These values were calculated by using (8) and (12) for curling and CS, respectively. The d_0 for the two-domain configuration was determined by using Amar's technique with the input parameters discussed in the previous section. The lower limit for d_0 derived by micromagnetics theory was calculated from (7) and is also given in Table 1.

The most obvious conclusion to be drawn from the results of Table 1 is that the two-domain configuration will not define the upper limit to SD behavior. For both the (100) and the (110) domain wall orientations, the predicted d_0 falls above the upper bound defined by micromagnetics. Thus the two-domain configuration can be eliminated as a possible upper limit to the SD range.

TABLE 1. Comparison of SD to Nonuniform Spin Transition
Diameters in Spherical Iron Particles

Nonuniform Spin Configuration	Predicted d_0,* Å	Reference
Two-domain plus 180° wall		Amar [1957, 1958a, b]
(100) wall	265	
(110) wall	225	
Magnetization curling	218†	Brown [1968]
Micromagnetics lower bound	167	Brown [1968]
CS	173	Morrish [1965, p. 342]

*Values for curling and CS calculated by using $A = 10^{-6}$ erg/cm.

†Micromagnetics upper bound.

Of the two remaining arrangements, CS predicts the lowest d_0 and is therefore the lowest-energy nonuniform configuration. The d_0 value predicted by CS easily falls between the bounds imposed by micromagnetics. The fact that CS satisfied the micromagnetics criterion gives us confidence that the calculations have been done correctly. These calculations strongly suggest that the upper limit to SD behavior in metallic iron will take place by transition to the CS configuration.

Since the value of the exchange constant A is in some dispute, it is instructive to investigate the implications of values of A other than the 10^{-6} erg/cm-value used for the calculations in Table 1. If $A = 0.5 \times 10^{-6}$ erg/cm, the lower bound for d_0 in spherical iron particles determined from (7) becomes 118 Å. The upper bound calculated by using $A = 0.5 \times 10^{-6}$ erg/cm in (8) would be 154 Å, whereas d_0 predicted by CS from (12) becomes 114 Å. If, on the other hand, $A = 2 \times 10^{-6}$ erg/cm (largest value reported), the lower and upper bounds become

236 and 307 Å, respectively. The CS would yield $d_0 = 260$ Å for $A = 2 \times 10^{-6}$ erg/cm. The experimental results of *Kneller and Luborsky* [1963] can be of some help in this matter. For dilute dispersions of fine iron spheres in mercury, a value of $d_0 = 220$ Å at 207°K was determined. This value is larger than the theoretical upper bound for d_0 if $A = 0.5 \times 10^{-6}$ erg/cm. Thus A must be greater than 0.5×10^{-6} erg/cm. Conversely, for $A = 2 \times 10^{-6}$ erg/cm, the theoretical lower bound to d_0 is greater than the experimental value, and A must be less than 2×10^{-6} erg/cm. Thus our initial choice of $A = 10^{-6}$ erg/cm is substantiated and will be used in the following calculations of d_0 for the SD to CS transition.

The results of calculating d_0 for the SD to CS transition as a function of temperature for spherical iron particles are shown in Figure 2. The temperature dependence of the exchange constant A was introduced in (12) by using the common and safe assumption that $A(T)/A(T_R) = J_s(T)/J_s(T_R)$, where $A(T)$ and $A(T_R)$ are the exchange constants at temperature T and at room temperature, respectively, and $J_s(T)$ and $J_s(T_R)$ are the saturation magnetizations at T and at room temperature, respectively. The temperature dependence of J_s was taken from *Bozorth* [1951, p. 112]. The value of d_0 is seen to increase with temperature, as has been suggested by *Kneller* [1969] and *Pearce* [1973]. Also shown in Figure 2 are the SP threshold sizes for $\tau_s = 100$ s and $\tau_s = 4 \times 10^9$ years. These d_s values were calculated by (4) with the K_1 versus T data of *Klein and Kneller* [1966]. Comparison of the calculated d_s and d_0 sizes (Figure 2) reveals that $d_s > d_0$ even at room temperature. This result is very interesting and somewhat surprising. The calculations indicate that there is no stable SD grain size range for spherical metallic iron particles. Using the highest reported value of A will increase d_0 to 260 Å. However, as was mentioned previously, this value of A is inconsistent with experimental data. Also shown in Figure 2 is the micromagnetics upper
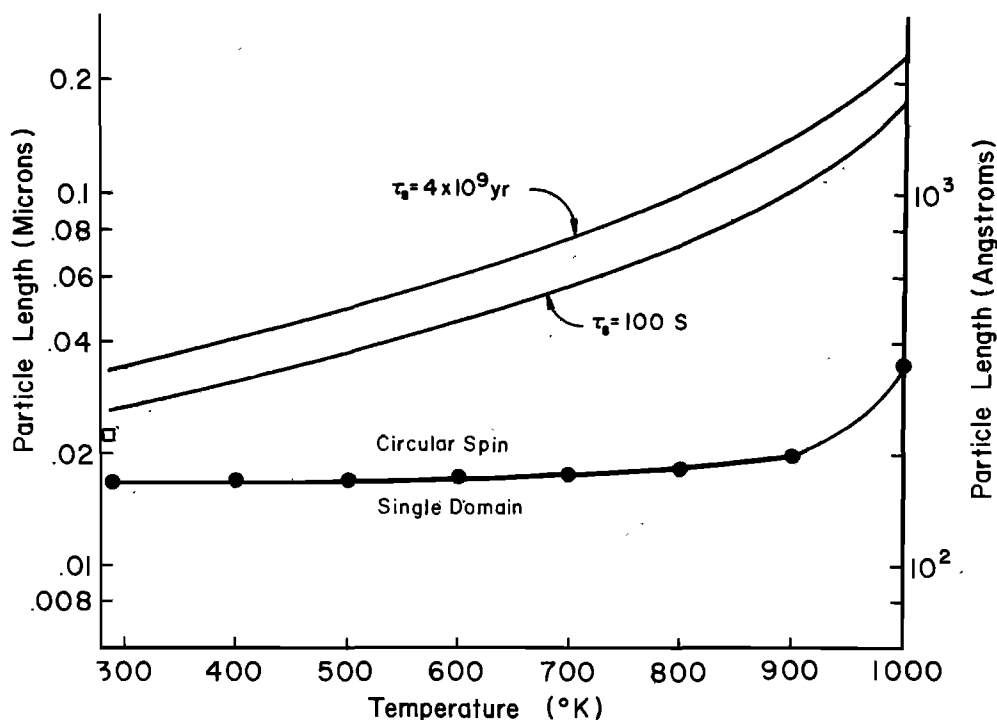

Fig. 2. Stable SD threshold diameters for spherical metallic iron particles. The SD to CS transition diameter is shown by the line through the solid circles and defines the upper limit to SD behavior d_0. Calculated SD to SP threshold diameters d_s for $\tau_s = 100$ s and 4×10^9 years are also shown. Here $d_s > d_0$ indicates that no stable SD range exists for spherical metallic iron particles. The micromagnetics upper bound for d_0 at room temperature is shown by the square.

bound for d_0 at room temperature. Although there can be some debate as to the exact nature of the nonuniform configuration that develops at d_0 (and therefore some uncertainty in d_0), the upper limit to SD behavior must be at or below the upper bound derived from micromagnetics. This upper bound could be raised to 307 Å by using $A = 2 \times 10^{-6}$ erg/cm. However, as was mentioned previously, acceptance of this high value of A amounts to neglecting the experimental d_0 determinations by *Kneller and Luborsky* [1963]. Since we cannot justify $d_0 > 218$ Å (micromagnetics upper bound for $A = 10^{-6}$ erg/cm), the only alternative for calculating a stable SD range for spherical metallic iron is to decrease the SP threshold d_s. This can be done only by increasing the anisotropy constant K_1 or decreasing the frequency factor f_0 in (4). As was pointed out previously, d_s is very insensitive to the exact value of f_0. Although a rigorous derivation of f_0 for cubic anisotropy and relaxation times of $> 10^{-6}$ s has not yet been accomplished [*Aharoni*, 1973], it is very unlikely that revision of f_0 will lead to a significant decrease in d_s. Also, the magnetocrystalline anisotropy data of *Klein and Kneller* [1966] are well accepted and not likely to be significantly revised. If magnetocrystalline anisotropy is the only source of coercivity in spherical iron particles, there seems to be no defensible way to increase K_1 in order to justify a decrease in d_s. Thus the inescapable conclusion seems to be that a stable SD grain size range does not exist for spherical iron particles at room temperature or above. We shall return to this point in the discussion.

Figure 3 shows the results of d_0 and l_s calculations for a prolate ellipsoid with a polar axis to equatorial axis ratio q of 1.67. Again, the SD to CS critical length was calculated by using (6). Comparison of d_0 and l_s shows the development of a definite grain size range between l_s and d_0 within which SD behavior is expected. Any iron particle whose shape and size fall within this range will be a very efficient and stable carrier of remanent magnetization. It should be noted that the grain sizes involved are very small and the SD range is very narrow. At room temperature the upper limit to SD behavior in a prolate ellipsoid of $q = 1.67$ will occur at a length of ~ 400 Å, whereas the lower limit will occur at a length of ~ 150 Å.

Results of the room temperature calculations of d_s and d_0 for prolate ellipsoids of various elongations are given in Figure 4 as a function of axial ratio. The axial ratio is expressed as the inverse of elongation, $1/q$. Spherical particles are on the right edge of Figure 4, and prolate ellipsoids of increasing elongation occur toward the left. The micromagnetics limits for spherical particles are also shown. Again, for spherical particles we see that $d_s > d_0$, and there is no stable SD range. As we move toward the left in Figure 4 (toward more elongated prolate ellipsoids), a definite SD grain size develops in which $d_0 > l_s$. However, even for very elongated particles, SD behavior occurs only in extremely small particles and within a very narrow range of grain size. For example, even for particles with elongation 5:1 ($1/q = 0.2$), SD behavior will occur only between particle lengths of $0.02 \le l \le 0.2 \mu$. The SD grain size range will decrease for all elongations with increasing temperature, as was observed in Figure 3.

It is important to mention here that we do not think that the CS configuration will persist for $d \gg d_0$. The CS is a less energetic configuration than SD for $d > d_0$ but is still a high-energy arrangement. It is logical to expect domain structure to develop in grains significantly above d_0. This transition from CS to domain structure would be likely to occur at ~ 100 Å above d_0. The succession of spin structures expected in fine metallic iron particles would then be (1) SP below d_s, (2) stable SD for $d_s < d < d_0$, (3) CS for $d_0 < d < d_0 + 100$ Å, and (4) domain structure. The development of domain structure above the CS grain size range implies the possible development of pseudo SD behavior in small multidomain (MD) iron grains. These pseudo SD grains could be significant carriers of remanent magnetism in lunar samples.

DISCUSSION AND CONCLUSIONS

Studies of the magnetic properties of lunar samples have recently been reviewed by *Fuller* [1974]. Examination of hysteresis quantities such as saturation magnetization (J_s), saturation remanence (J_r), bulk coercive force (H_c), remanence coercivity (H_{rc}), and initial susceptibility (χ_0) have aided in the characterization of the samples [*Nagata et al.*, 1972]. In
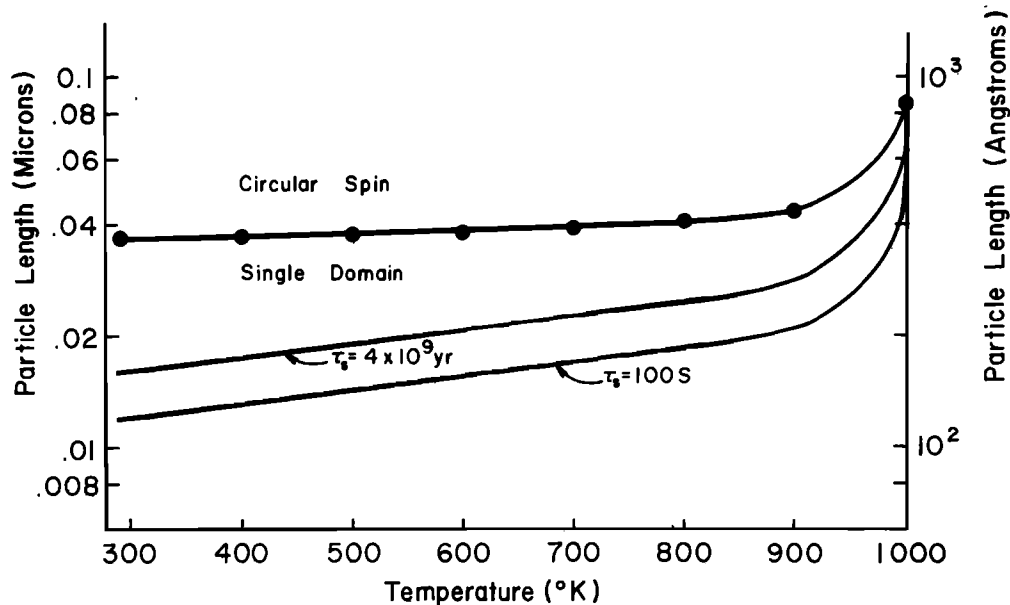

Fig. 3. Stable SD threshold lengths for an iron prolate ellipsoid of elongation $q = 1.67$. The SD to SP threshold lengths l_s for $\tau_s = 100$ s and 4×10^9 years are shown by the two lower curves. The upper limit to the SD range, d_0, is defined by the SD to CS transition and is shown by the line through the solid circles. A definite stable SD grain size range exists between l_s and d_0.
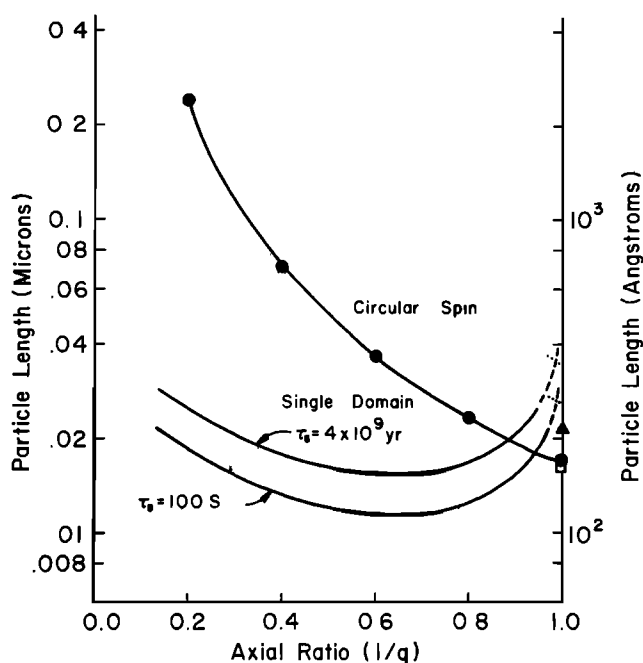
Fig. 4. Stable SD grain size range for iron prolate ellipsoids at room temperature (290°K) as a function of axial ratio. The axial ratio is given as the inverse of elongation, so that spherical particles appear on the right edge of the diagram and elongated particles are shown toward the left. The SD to CS transition is shown by the line through the solid circles. The SP threshold lengths l_s are shown for $\tau_s = 100$ s and 4×10^9 years. The dashed portions of the l_s lines indicate the SP threshold length if shape anisotropy is the only source of coercive force. The dotted portions illustrate the SP critical length if magnetocrystalline anisotropy is the only source of coercivity. In reality, the dashed and dotted portions will be smoothly connected. The exact shape of the l_s lines in this region will depend on the crystallographic direction of particle elongation. The micromagnetics upper (solid triangle) and lower (open square) bounds for d_0 are also shown for spherical particles.

general, the dominant magnetic mineral is metallic iron, and low J_r/J_s ratios indicate that only a small proportion of this iron is in the stable SD range. The majority of the metallic iron is present as SP or MD grains.

Lunar soil samples contain an average of 0.5% metallic iron. Hysteresis properties measured at various temperatures indicate that a large proportion of the iron particles are SP [Nagata and Carleton, 1970]. Breccia samples also contain about 0.5% metallic iron but display hysteresis properties that are a function of the degree of annealing (metamorphism) [Gose et al., 1972]. The least-annealed samples are a mixture of very fine SP and SD particles, whereas the most severely metamorphosed samples are dominated by MD behavior. This transition in the magnetic properties of the breccias is an apparent reflection of grain growth during annealing [Pearce et al., 1972]. Both breccias and soils commonly exhibit large components of viscous magnetization [Gose et al., 1972; Nagata et al., 1972]. Lunar igneous rocks contain ~0.1% metallic iron that is predominantly MD.

Results of the present investigation may help to explain some of these properties. The basic results of our investigation of stable SD grain size limits in metallic iron are twofold: (1) there is no stable SD range for spherical particles, and (2) only very small elongated iron grains ($q > 1.1$, $150 < d < 600$ Å) will have a stable SD range, and this range will be extremely narrow. Fine particles of metallic iron will tend to form as spherical particles in order to minimize their surface to volume

ratio. Thus it is not surprising that only a small proportion of the iron grains in lunar soils satisfy both the size and the shape criteria required for them to fall within the stable SD range (Figure 4). The small average grain size in lunar soils and soillike breccias (100–300 Å) [Housley et al., 1973] and the proximity of d_s and d_0 for spherical or slightly elongate particles ($q < 1.1$) may also explain the widespread occurrence of viscous magnetization in these samples.

It is interesting to note that the frequently assumed 150- to 300-Å-diameter SD range for spherical iron particles is in conflict with experimental data. Observation of the size distribution of metallic iron spheres in glass-welded aggregates by Housley et al. [1973] has revealed that 100- to 250-Å spheres dominate the distribution. Approximately 30% of the metallic iron is in the 150- to 300-Å range. If this distribution is representative of the iron grain size distributions for soils and low metamorphic grade breccias, the 150- to 300-Å stable SD range would predict a saturation isothermal remanence (IRM_s) of >1 emu/g. However, the largest IRM_s values observed are less than 10^{-1} emu/g [Fuller, 1974, Figure 28], and assumption of the 150- to 300-Å SD range leads to a direct conflict with the experimental data.

The magnetic granulometry experiments on lunar breccia 14313 by Dunlop et al. [1973] are very interesting in the context of the present SD grain size calculations. A grain size versus coercive force distribution was determined for 14313,29 by partial thermoremanence and af demagnetization experiments. The distribution is illustrated by Dunlop et al. [1973, Figure 5]. The main peak in the distribution at a coercivity of ~1000 Oe is undoubtedly due to elongate SD metallic iron. However, the distribution also exhibits a truncation below coercive forces of 300–500 Oe. Dunlop et al. [1973] attribute this truncation to a minimum coercivity due to magnetocrystalline anisotropy for spherical SD particles. Thus the magnetic granulometry of 14313,29 appears to require stable SD spherical iron grains, a result that conflicts with the present calculations. There are two possible explanations for the apparent conflict.

One possibility is that the grain shape distribution is heavily skewed in favor of spherical grains rather than elongate grains. Such a skewed distribution would, in fact, be predicted by the tendency of fine iron particles to minimize the surface to volume ratio. The combination of the expected grain shape distribution with our result that grains with an elongation of <1.1 do not possess a stable SD grain size range would yield the truncation effect observed by Dunlop et al. [1973]. The second possible explanation of the apparent conflict between the magnetic granulometry data for 14313,29 and our theoretical results is that a stable SD range does, in fact, exist. We are confident that our calculations are numerically correct and, as was discussed previously, that d_0 cannot be raised above 218 Å by any justifiable adjustment of the input parameters. The only recourse is to decrease d_s by speculating that magnetocrystalline anisotropy is not the only source of coercivity in the fine iron grains of lunar samples. Two conceivable sources of additional anisotropy would be (1) an increase in magnetocrystalline anisotropy by the alloying of the iron with highly anisotropic impurities such as cobalt or (2) magnetostrictive effects due to coherent strain in these extremely fine grained iron particles. Both of these mechanisms for increasing the effective anisotropy constant are highly speculative. Thus we favor the first explanation of the magnetic granulometry data for lunar breccia 14313,29.

Examination of the stable SD field (Figure 4) can also aid in understanding the transition in the magnetic behavior of brec-

cias during annealing and attendant grain growth. Least-annealed breccias will have a grain size and shape distribution similar to those for soils. Since no stable SD range exists for spherical particles and since the iron grains in the soils and low metamorphic grade breccias are thought to be spherical, the increase in the SD content of intermediate metamorphic grade breccias cannot take place simply by growth of SP iron spheres, as was proposed by *Pearce et al.* [1972]. However, sintering of adjacent spherical SD grains to yield elongated SD particles during the short-time and/or low-temperature annealing experienced by intermediate metamorphic grade breccias would produce the increased SD content observed. Continued annealing at higher temperatures would yield larger grains with $d > d_0$ and favor formation of spherical iron particles. Thus severe annealing would result in predominantly MD grains, such as those observed in highly metamorphosed breccias.

Cisowski et al. [1973] have observed an increase in H_c and the J_r/J_s ratio of breccias during laboratory shock experiments. They interpret these changes as an increase in the proportion of stable SD iron grains and suggest deformation of originally spherical particles during shock as the explanation. As is illustrated by Figure 4, our results indicate that deformation of 100- to 400-Å-diameter spheres to produce prolate ellipsoids of elongation $q > 1.1$ would indeed produce a substantial increase in the stable SD content of shocked breccias.

We have stressed the constricted nature of the stable SD grain size range and have attempted to explain a number of observations of magnetic properties of lunar samples on the basis of the low probability of finding metallic iron particles within the stable SD field. It is therefore essential to establish that only a small proportion of stable SD particles are required to account for the NRM's of high stability that have been observed in some lunar breccias and igneous rocks. The largest IRM$_s$ reported for breccias and igneous samples are approximately $0.5 \times 10.^{-1}$ emu/g [*Fuller*, 1974, Figure 28]. For an assemblage of randomly oriented stable SD particles with uniaxial anisotropy, IRM$_s$ is $(J_s/2)$ emu/g of ferromagnetic material. The percentage of the metallic iron content that must be present as stable SD's in order to account for a given IRM$_s$ in a rock would be

$$\% \text{ SD} = \{(\text{IRM}_s)/[(\text{fraction Fe})(J_s/2)]\} \times 100\% \quad (13)$$

For metallic iron in lunar samples, $J_s = 220$ emu/g and the fraction of iron is $\simeq 0.005$. Thus (13) yields % SD $\simeq$ 9% for the highest values of IRM$_s$, and at most, only 9% of the metallic iron present is required to be in the stable SD range. This calculation neglects the contribution of MD grains to IRM$_s$. The contribution from MD grains may be considerable, and the 9% SD figure is an upper limit even for the lunar samples with the strongest IRM$_s$. These calculations illustrate that the NRM of lunar breccias and igneous samples can be accounted for by a very small stable SD content. Since it is very likely that 1–10% of the iron particles in lunar samples would be sufficiently elongate to fall within the SD bounds in Figure 4, the results of our theoretical calculations are not in conflict with the observations of stable NRM in some lunar samples.

As was mentioned previously, calculations of SD grain size limits for metallic iron are also important in evaluating the iron-silicate fractionation mechanism of *Harris and Tozer* [1967]. The magnetostatic interaction mechanism proposed by *Harris and Tozer* [1967] applies only to interaction between SD particles. Since neither K_1 nor J_s is significantly affected by

the alloying of a small percentage of Ni with Fe, the SD limits for the 5% Ni alloys found in chondritic meteorites will be virtually identical to those of metallic iron. *Larimer and Anders* [1970] have examined the abundances of volatile siderophile elements in chondritic meteorites in order to estimate the temperature range in which the iron-silicate fractionation occurred. These temperature limits are approximately $680° < T < 1050°\text{K}$. As was indicated in Figure 3, the stable SD range becomes narrower with increasing temperature. Thus the requirements of grain shape and size for SD behavior shown for room temperature (Figure 4) will be even more confining in the temperature region of iron-silicate fractionation. Given the size and shape requirements for stable SD behavior (Figure 4), we consider it unlikely that a significant proportion of the metal grains in the solar nebula would be in the SD region. Thus we do not consider magnetostatic interaction between metal grains in the solar nebula to be a likely mechanism for iron-silicate fractionation.

If the appearance of ferromagnetism in the metal phase did trigger the fractionation, it appears most likely that the mechanism must involve the magnetic susceptibility contrast between metals and silicates rather than the magnetostatic interaction of metal grains. The magnetic susceptibility of metallic iron is much larger than the susceptibility of silicates. Thus metal grains in the solar nebula would experience a much stronger translational force due to a magnetic field gradient than silicate particles would. Although evidence does exist for the presence of a magnetic field at the time of accretion of carbonaceous chondrites [*Banerjee and Hargraves*, 1972; *Brecher*, 1972; *Butler*, 1972], the existence of magnetic field gradients sufficient for an effective separation of metal and silicate particles is purely speculative. However, local intensification of magnetic lines of flux in a turbulent condensing solar nebula may have produced the required magnetic field gradient.

REFERENCES

Aharoni, A., Relaxation time of superparamagnetic particles with cubic anisotropy, *Phys. Rev., 7*, 1103–1107, 1973.

Amar, H., On the width and energy of domain walls in small multi-domain particles, *J. Appl. Phys., 28*, 732–733, 1957.

Amar, H., Size dependence of the wall characteristics in a two-domain iron particle, *J. Appl. Phys.*, 542–543, 1958a.

Amar, H., Magnetization mechanism and domain structure of multi-domain particles, *Phys. Rev., 111*, 149–153, 1958b.

Banerjee, S. K., Fractionation of iron in the solar system, *Nature, 216*, 781, 1967.

Banerjee, S. K., and R. B. Hargraves, Natural remanent magnetizations of carbonaceous chondrites and the magnetic field in the early solar system, *Earth Planet. Sci. Lett., 17*, 110–119, 1972.

Bean, C. P., and J. D. Livingston, Superparamagnetism, *J. Appl. Phys., 30*, 120S–129S, 1959.

Bozorth, R. M., *Ferromagnetism*, 968 pp., Van Nostrand, Princeton, N. J., 1951.

Brecher, A., Memory of early magnetic fields in carbonaceous chondrites, in *Proceedings of the Nice Symposium on the Origin of the Solar System*, pp. 260–273, Centre National de Recherche Scientifique, Paris, 1972.

Brown, W. F., Jr., Thermal fluctuations of a single-domain particle, *Phys. Rev., 130*, 1677–1686, 1963.

Brown, W. F., Jr., The fundamental theorem of fine-ferromagnetic-particle theory, *J. Appl. Phys., 39*, 993–994, 1968.

Butler, R. F., Natural remanent magnetization and thermomagnetic

properties of the Allende meteorite, *Earth Planet. Sci. Lett., 17,* 120–128, 1972.

Butler, R. F., and S. K. Banerjee, Theoretical stable single-domain grain size range in magnetite, submitted to *J. Geophys. Res.,* 1975.

Chikazumi, S., *Physics of Magnetism,* 554 pp., John Wiley, New York, 1964.

Cisowski, C. S., M. Fuller, M. F. Rose, and P. J. Wasilewski, Magnetic effects of explosive shocking of lunar soil, *Proc. Lunar Sci. Conf. 4th, 3,* 3003–3017, 1973.

Dunlop, D. J., Magnetite: Behavior near the single-domain threshold, *Science, 176,* 41–43, 1972.

Dunlop, D. J., Superparamagnetic and single-domain threshold sizes in magnetite, *J. Geophys. Res., 78,* 1780–1793, 1973.

Dunlop, D. J., and G. F. West, An experimental evaluation of single-domain theories, *Rev. Geophys. Space Phys., 7,* 709–757, 1969.

Dunlop, D. J., W. A. Gose, G. W. Pearce, and D. W. Strangway, Magnetic properties and granulometry of metallic iron in lunar breccia 14313, *Proc. Lunar Sci. Conf. 4th, 3,* 2977–2990, 1973.

Evans, M. E., Single-domain particles and TRM in rocks, *Comments Earth Sci. Geophys., 2,* 139–148, 1972.

Frei, E. H., S. Shtrikman, and D. Treves, Critical size and nucleation field of ideal ferromagnetic particles, *Phys. Rev., 106,* 446–455, 1957.

Fuller, M., Lunar magnetism, *Rev. Geophys. Space Phys., 12,* 23–70, 1974.

Gose, W. A., G. W. Pearce, D. W. Strangway, and E. E. Larson, Magnetic properties of Apollo 14 breccias and their correlation with metamorphism, *Proc. Lunar Sci. Conf. 3rd, 3,* 2387–2395, 1972.

Grommé, C. S., and R. R. Doell, Magnetic properties of Apollo 12 lunar samples 12052 and 12062, *Proc. Lunar Sci. Conf. 2nd, 3,* 2491–2499, 1971.

Grossman, L., and J. W. Larimer, Early chemical history of the solar system, *Rev. Geophys. Space Phys., 12,* 71–101, 1974.

Harris, P. G., and D. C. Tozer, Fractionation of iron in the solar system, *Nature, 215,* 1449–1451, 1967.

Housley, R. M., R. W. Grant, and N. E. Paton, Origin and characteristics of excess Fe metal in lunar glass welded aggregates, *Proc. Lunar Sci. Conf. 4th, 3,* 2737–2749, 1973.

Kittel, C., Physical theory of ferromagnetic domains, *Rev. Mod. Phys., 21,* 541–583, 1949.

Klein, H. P., and E. Kneller, Variation of magnetocrystalline

anisotropy of iron with field and temperature, *Phys. Rev., 144,* 372–374, 1966.

Kneller, E., Fine particle theory, in *Magnetism and Metallurgy,* edited by E. A. Berkowitz and E. Kneller, pp. 365–471, Academic, New York, 1969.

Kneller, E., and E. E. Luborsky, Particle size dependence of coercivity and remanence of single-domain particles, *J. Appl. Phys., 34,* 656–658, 1963.

Larimer, J. W., and E. Anders, Chemical fractionations in meteorites, 3, Major element fractionations in chondrites, *Geochim. Cosmochim. Acta, 34,* 367–387, 1970.

Lilley, B. A., Energies and widths of domain boundaries in ferromagnetics, *Phil. Mag., 41,* 792–813, 1950.

Morrish, A. H., *The Physical Principles of Magnetism,* 680 pp., John Wiley, New York, 1965.

Nagata, T., and B. J. Carleton, Natural remanent magnetization and viscous magnetization of Apollo 11 lunar materials, *J. Geomagn. Geoelec., 22,* 491–506, 1970.

Nagata, T., R. M. Fisher, and F. C. Schwerer, Lunar rock magnetism, *Moon, 4,* 160–186, 1972.

Néel, L., Some theoretical aspects of rock-magnetism, *Phil. Mag. Suppl., 4,* 191–243, 1955.

Pearce, G. W., Magnetism and lunar surface samples, Ph.D. thesis, Univ. of Toronto, Toronto, Ont., Canada, 1973.

Pearce, G. W., R. J. Williams, and D. S. McKay, The magnetic properties and morphology of metallic iron produced by subsolidus reduction of synthetic Apollo 11 composition glasses, *Earth Planet. Sci. Lett., 17,* 95–104, 1972.

Stoner, E. C., Ferromagnetism: Magnetization curves, *Rep. Prog. Phys., 13,* 83–183, 1950.

Strangway, D. W., W. A. Gose, G. W. Pearce, and J. G. Carnes, Magnetism and the history of the moon, 18th Annual Conference on Magnetism and Magnetic Materials, *Amer. Inst. Phys. Conf. Proc., 10,* 1178–1196, 1972.

Wohlfarth, E. P., Energy of a Bloch wall on the band picture, *Proc. Phys. Soc. London, Ser. A, 65,* 1053–1054, 1952.